PROCEEDINGS, 49th Workshop on Geothermal Reservoir Engineering
Stanford University, Stanford, California, February 12-14, 2024
SGP-TR-227

Tracer Response and Evaluation of Thermal Front Migration at an Operating Geothermal Field in the Western USA

Zachary Brown, Leland Davis, Alexander Milton

Geologica Geothermal Group

75 Caliente Street, Reno, NV 89509

zbrown@geologica.net

Keywords: Tracer Test, Permeability, Thermal Front Migration

ABSTRACT

A long-term reservoir tracer test using conservative naphthalene-di-sulfonate (NDS) type tracers was performed in early 2022 at a known geothermal resource area (KGRA) and operating geothermal field in the Basin and Range Province of the Western United. Unique tracers were injected into four separate injection wells (I-1, I-2, I-3, I-4). Production wells (P-1, P-2, P-3, P-4, P-5) were monitored for tracer returns for a period of ~130 days. Results of this tracer test confirmed strong permeable connections between all production wells and injection wells I-1 and I-4 in the central geothermal reservoir area and established the connection of northern injection wells I-2 and I-3 to the main reservoir via returns in P-2, P-3, and P-4. Tracer return data of sufficient quality was used to estimate mean residence times of injected fluid and to characterize swept pore volume, flow geometry (heterogeneity), sweep efficiency, and thermal front migration times for production-injection pairs. Interpretation of the tracer test results has informed the current understanding of flow pathways and connections in the KGRA and is constrained with recent and historic operational data from the wellfield. Additionally, comparisons of estimated thermal front migration times to observed thermal decline from downhole temperature logs has confirmed the reliability of these calculations and their usefulness in predicting thermal impacts of production and injection regimes.

INTRODUCTION

In early 2022 a reservoir tracer test using conservative naphthalene-di-sulfonate (NDS)-type tracers was performed at a known geothermal resource area (KGRA) and operating geothermal field in Basin and Range Province of the Western United States. The goal of the tracer study was to assess fluid flow pathways and characteristics, and better define the connections of injecting wells and production wells for reservoir management. The tested geothermal resource has supported power generation for ~40 years via a steam turbine unit and a secondary binary plant which came online in 2007. During this time reservoir pressure and temperature decline has been monitored based on periodic downhole pressure and temperature (PT) surveys during shut-in periods for production and injection wells. In 2018 new production well P-5 and new injection well I-4 came online; the present study was undertaken to track reservoir response to long term exploitation over time and to track the reservoir response to changes in operations.

Currently, there are five operating production wells in the field (P-1, P-2, P-3, P-4, P-5) and four injection wells (I-1, I-2, I3, I4). Two injection wells, I-2 and I-3, considered to be minimally or not at all connected to the main reservoir, are used intermittently at relatively low flow rates (Figure 1). Between 2019 – 2022 annual geochemical monitoring of the operating production wells and injection fluids and new PT logs in each well have allowed for investigation of the typical geothermal reservoir responses to continued exploitation of the geothermal resource (e.g. cooling and pressure drawdown). Data from geochemical monitoring indicates conservative elements such as chloride (Cl) have increased in reservoir fluids over time while dissolved silica concentrations and measured temperatures have decreased, suggesting the majority of cooling within the geothermal field is due to re-injection breakthrough and not cold meteoric water recharge. Geochemical markers of cold meteoric waters such as bicarbonate (HCO_3) and magnesium (Mg) have also remained at relatively steady concentrations over time consistent with cooling unrelated to cool meteoric water influx. However, as the relative flow paths, velocity, and connections between production and injections wells are not well understood questions remain as to how and why this geothermal reservoir has sustained operations relatively minimal (~20 - 30°C) cooling over time and what effect new wells (I-4 and P-5) may have on the reservoir moving forward.

The study below reports the findings from a recent tracer test and its implications for further exploitation of the geothermal resource by examining thermal front migration times between production and injection pairs estimated from tracer returns times. These thermal front migration times are compared to available operational datasets (PT logs, production and injection rates, etc.) to evaluate the reliability of the thermal front migration calculations and the usefulness of these calculations in understanding and predicting temperature changes in the geothermal field over time.

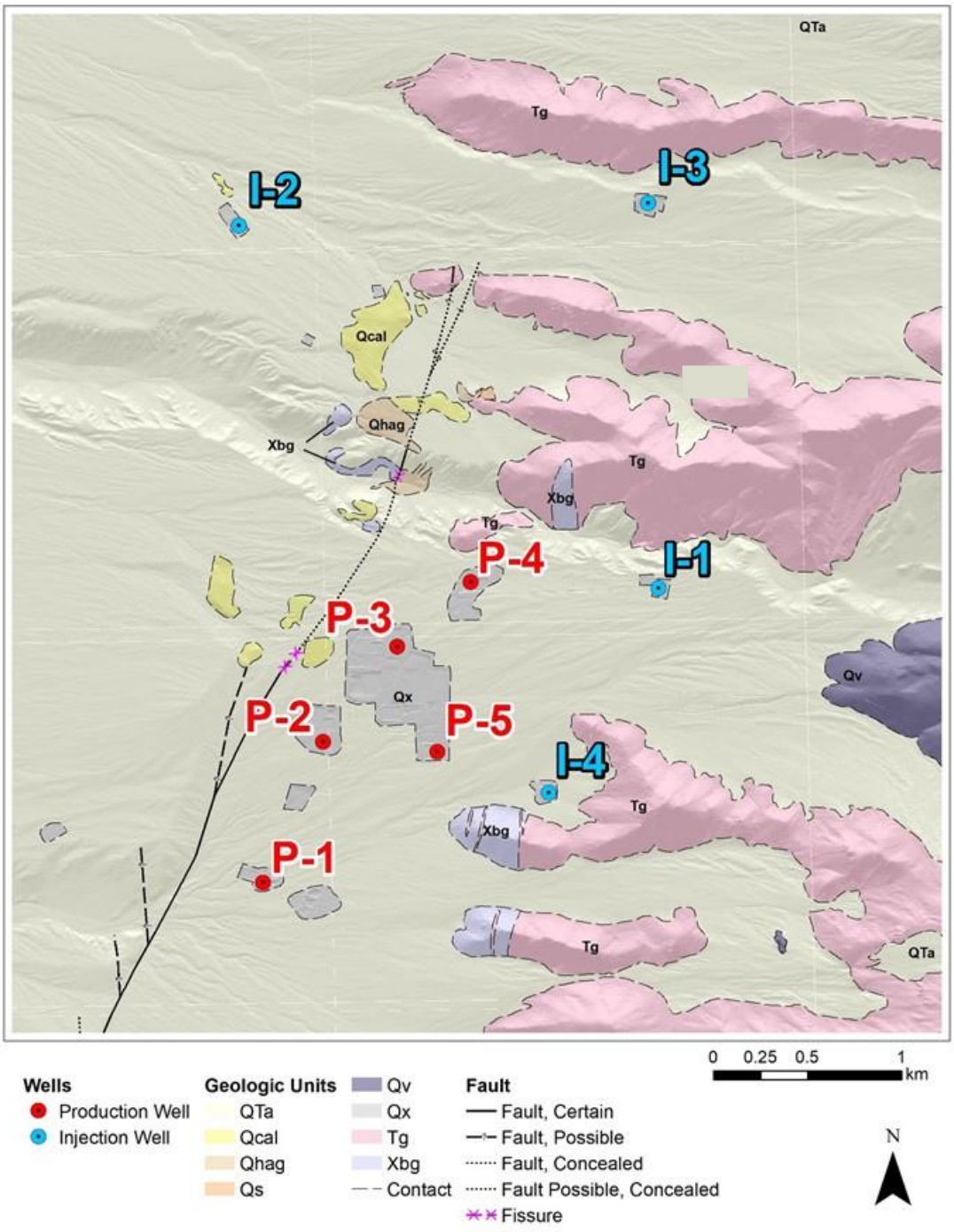

Figure 1. Map of the geothermal wellfield showing surface geology, well location, and operational use.

TRACER TEST PLAN AND IMPLEMENTATION

Four unique tracers were injected into four separate injection wells (I-1, I-2, I-3, I-4) in early January 2022 and production wells (P-1, P-2, P-3, P-4, P-5) were monitored for tracer returns for a period of ~130 days. Injection wells, I-1 and I-3, were also monitored for tracer to determine when produced fluid was recycled (re-injected) after first detection in production wells. Tracer samples from production and injection wells were recorded and catalogued at the time they were taken and these samples were shipped in batches to the Earth & Geoscience Institute (EGI) at the University of Utah in Salt Lake City, Utah for laboratory analysis. Table 1 shows the specific tracer injected into each well and associated operational data.

Table 1. Tracer injection data and injection well conditions for the 2022 tracer test.

Well	Chemical Tracer	WHP	WHT	Injection Flow Rate (Monthly Avg)
		barg	°C	metric tons per hour (tph)
I-1	1,5 NDS	4.08	85.6	699
I-2	2,7 NDS	0	88.3	51
I-3	1 NDS	2.72	90.6	39
I-4	2,6 NDS	0.34	82.2	208

TRACER TEST FINDINGS

Tracer Data Discussion

Tracer testing and analysis methods generally assume production and injection conditions are steady throughout the test, and the results of the tracer test only apply to the specific operational conditions during that period. Changes in well use, such as increasing injection/production rates may change the conditions in the reservoir and therefore affect the accuracy of tracer test results and analytical methods used to assess tracer test data. During the tracer testing time period there was a shift in injection beginning in March 2022, with flow increasing in I-4 and decreasing in I-1 associated with scaling and physical flow restriction in I-1 (Figure 2). Injection into the two northern injectors I-2 and I-3 was also sporadic during the tracer testing period, which led to inconsistent tracer detections from those wells (Figure 2). Production flow rates were steady over the first 5 months of the tracer test period except in P-1which was shut-in in June of 2022 ~1 month before the end of tracer sampling (Figure 2). Therefore, the results of the tracer test should be viewed in context of changing operational conditions during the tracer test period.

Table 2 displays tracer detection times for first tracer detection and peak tracer concentration for the 2022 tracer test. Figures 3 – 6 show the tracer return curves of tracer injected into injection wells I-1, I-2, I-3, and I-4. It should be noted that the magnitude of tracer returns shown on the Y-axis of the plots below varies greatly as tracer returns in different wells ranged widely from maximum values of ~1.5 – 120 ppb.

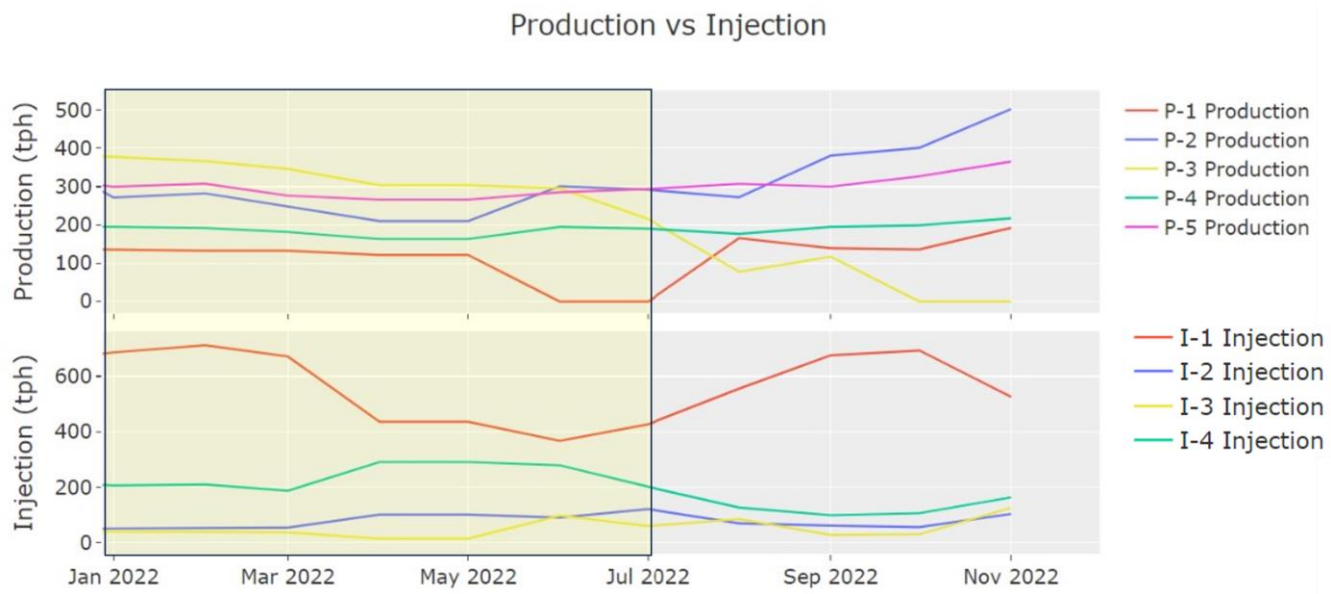

Figure 2. Available production and injection flow in metric tons per hour (tph) for the 2022 tracer test period with the 2022 tracer test period highlighted.

Table 2. Tracer detection times for first and peak returns. Dash marks indicate that no tracer returns were observed during the tracer sampling period.

Injection Well	Chemical Tracer	P-1 First Return	P-1 Peak Return	P-2 First Return	P-2 Peak Return	P-3 First Return	P-3 Peak Return	P-4 First Return	P-4 Peak Return	P-5 First Return	P-5 Peak Return
		Days									
I-1	1,5 NDS	47	103*	26	75	16	59 - 75^	16	47	11	75
I-2	2,7 NDS	-	-	75	103*	75	132*	18	31	7	8
I-3	1 NS	-	-	75	132*	68	132*	68	68*	-	-
I-4	2,6 NDS	33	82	18	47	10	26 - 59^	10	31	6	13
* = Max concentration but peak and decline not observed											
^ = Peak data correlates with change in flow rate											

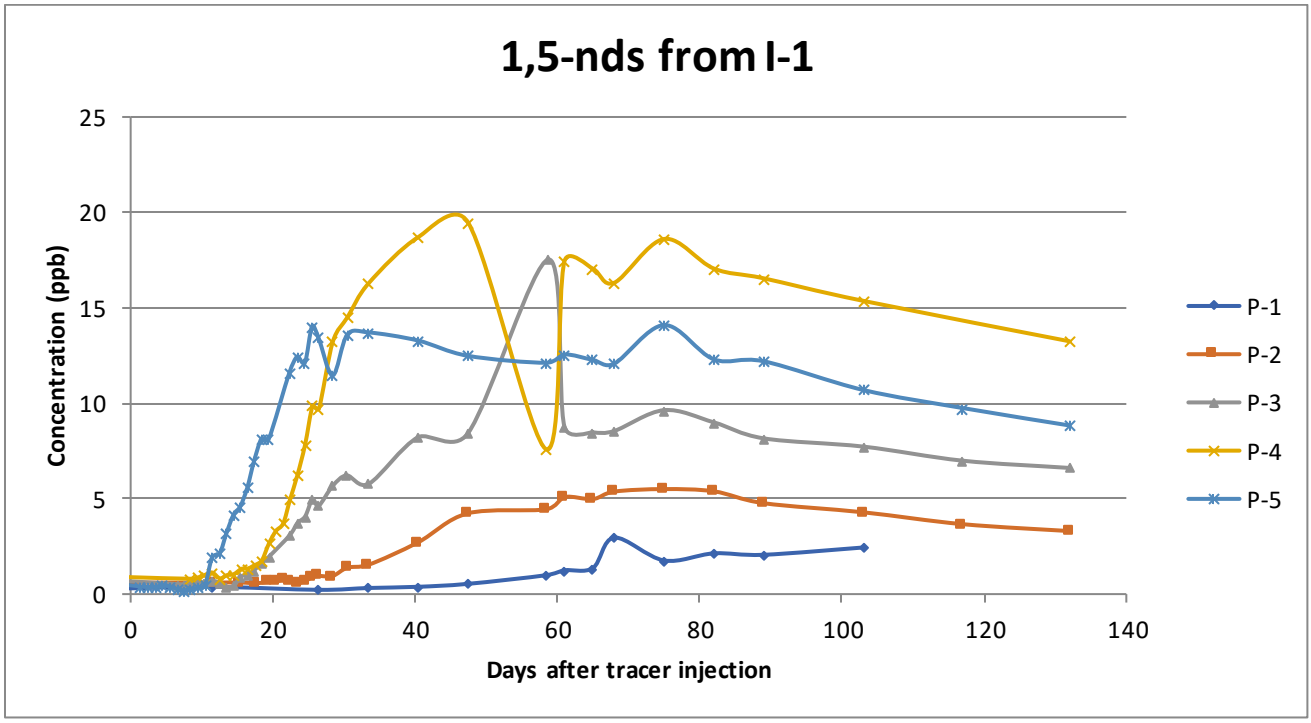

Figure 3. Analytical tracer returns curves for 1,5 NDS injected into I-1. Tracer was returned from all production wells in the wellfield.

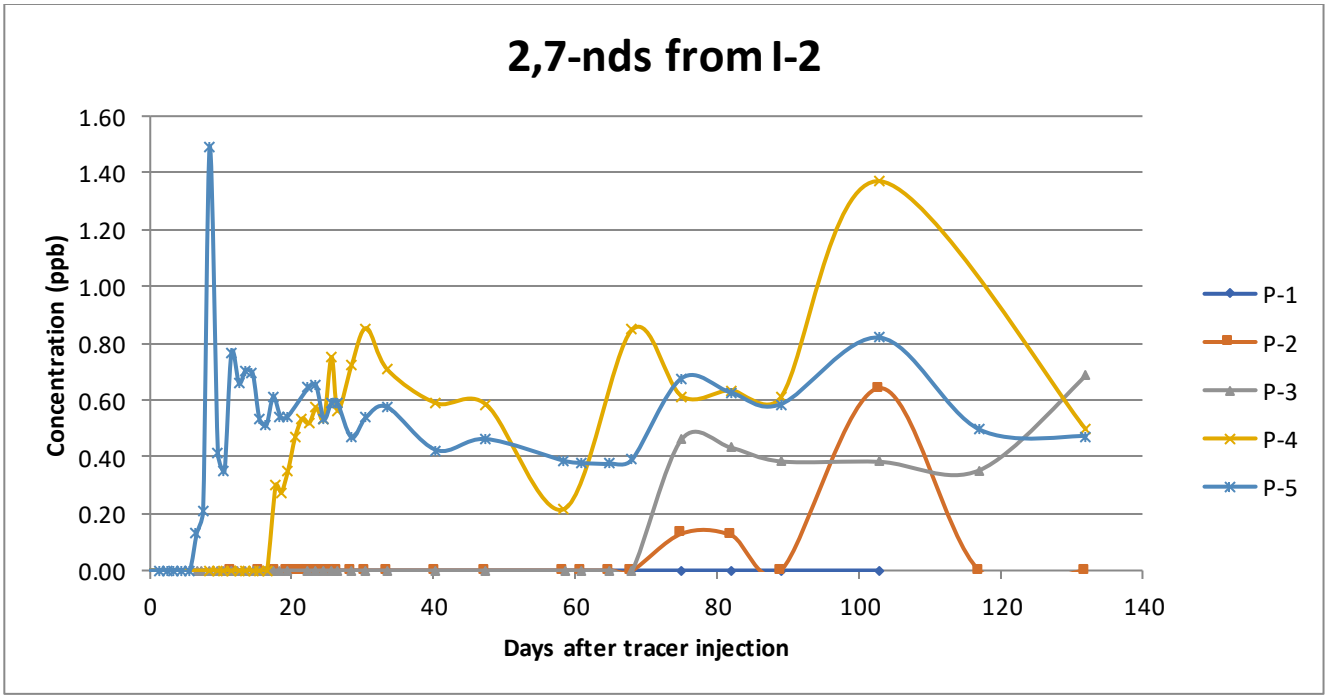

Figure 4. Analytical tracer returns curves for 2,7 NDS injected into I-2. Tracer returns were observed in all production wells expect P-1.

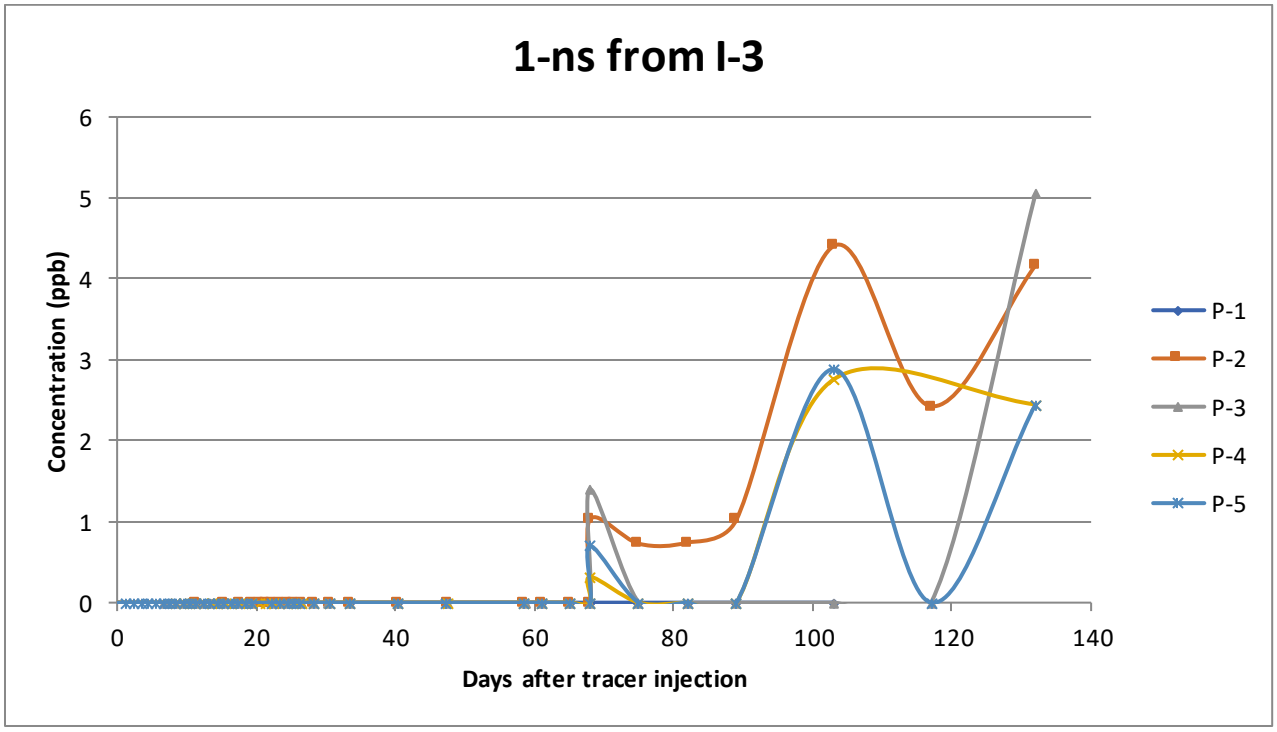

Figure 5. Analytical tracer returns curves for 1 NS injected into I-3. Tracer returns were observed in all production wells expect P-1.

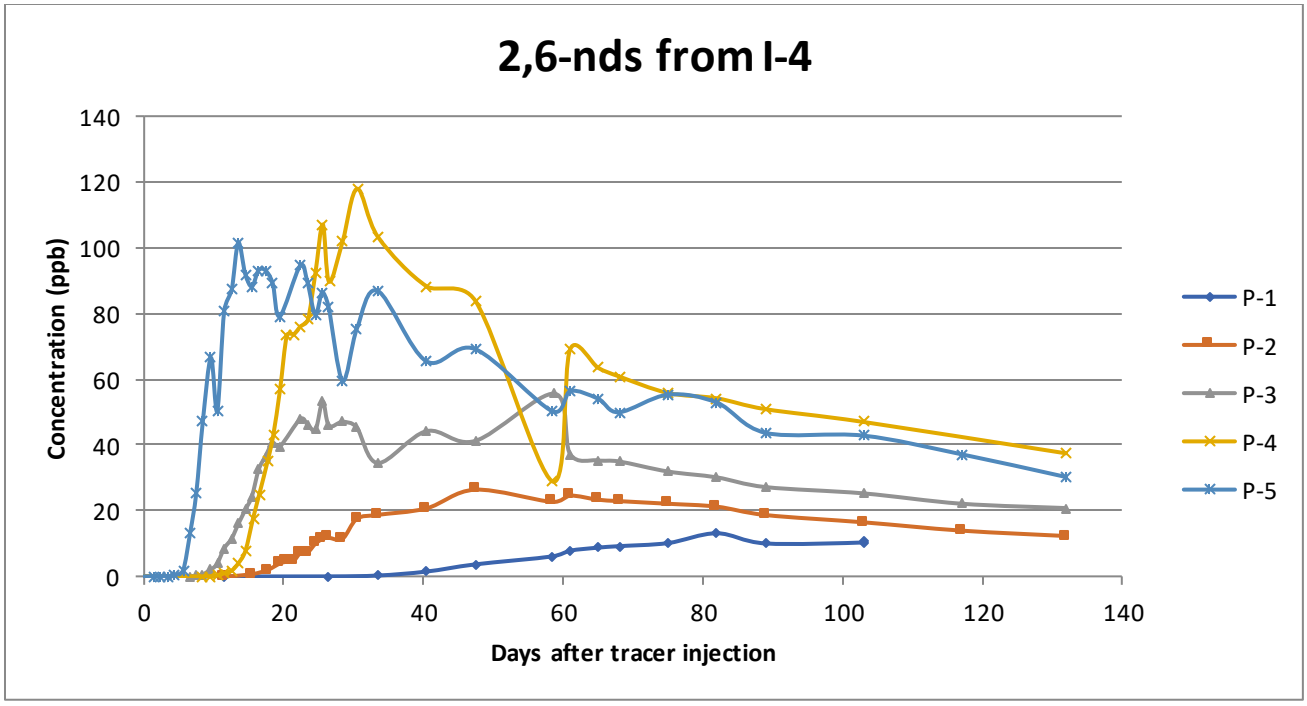

Figure 6. Analytical tracer returns curves for 2,6 NDS injected into I-4. Tracer was returned from all production wells in the wellfield.

Analytical Tracer Data Evaluation

The tracer test data collected from the 2022 test were evaluated by the timing and magnitude of the tracer returns measured in each production well. When a significant peak and declining period were observed, the tracer results were also analyzed using the methods outlined in Shook & Forsman (2005) to determine the first temporal moment of a tracer. This method includes the following steps:

- Interpolation of tracer curves from the reported data (which has irregular time intervals) to 1-day time steps.
- Conversion of the interpolated reported tracer concentration (units ppb) to a normalized age distribution (units 1/day).
- De-convolution of tracer to account for re-injection / re-circulation of tracer throughout the test (see below).
- Extrapolating the attenuation rate beyond the current monitoring period based on exponential decline.
- Calculating the mean residence time (first temporal moment (T*).
- Calculating the pore volume swept by injection between well pairs.

Once the first temporal moment is determined, the normalized tracer data and injection rate are used to estimate:

- Flow geometry (heterogeneity),
- Sweep efficiency,
- Thermal front migration times.

Shook & Forsmann (2005) give analytical solutions based on tracer return curves and make two major assumptions; 1.) a steady state (constant) injection and production between well pairs and 2.) that the tracers used are ideal and conservative, meaning they are not absorbed or decayed during the period of the tracer test. As noted above, the operational conditions during this tracer test were not perfectly constant and therefore the results of this analysis should be viewed with this in mind. Furthermore, this method assumes that the injection (and recycling) of any single tracer is through only one single injection well, which is not true for this test as tracer was re-injected (recycled) through all operating injection wells after the first return of tracer though at differing flow rates as shown in Figure 2. Therefore, specific values of reservoir characteristics such as mean residence time, thermal front migration time, etc. derived from analytical methods should be viewed in context of changing operational conditions during the tracer test and used as informed estimates of reservoir characteristics.

A summary of the characteristics determined via methods in Shook & Forsmann (2005) for all well pairs is shown in Table 3. Further discussion of the reservoir characteristics other than mean residence time (first temporal moment (T*)) and swept pore volume (Vp) follows below.

Flow Geometry (Heterogeneity)

The analysis of flow geometry is dependent on late-time data (collected during tracer attenuation and extrapolated after the last available sample), as a measure of the full distribution of permeable space. Flow (geometry) heterogeneity is a relation of the flow capacity of fractures versus the pore volume and is described in Shook (2001). The method offers a qualitative understanding of the variations in flow capacity of reservoir fractures but cannot be used to determine the spatial distribution of these properties. A higher proportion of flow capacity relative to storage indicates some fractures have higher fluid velocity, and the overall distribution is more heterogenous compared to homogeneous where all fractures or permeable space have the same flow capacity relative to storage (Figure 7). Conversely, an even amount of flow capacity and storage indicates fractures have a more uniform permeability and the overall distribution is less heterogenous. While some heterogeneity occurs in all natural systems, a more homogenous connection between production and injection well pairs can limit potential rapid injection breakthrough.

Flow and storage capacity were determined and plotted for well pairs with sufficient data in Figure 7. As expected, these well pairs are have varying degrees of heterogeneity due to natural variation, however all well pairs indicate flow in the geothermal reservoir is within fractured non homogenous media as expected for a fault-controlled system.

Sweep Efficiency

Volumetric sweep efficiency describes the amount of pore volume contacted by the injection fluid relative to the overall reservoir pore volume estimated from the tracer return data. It is a measure of how efficient injection fluids are at sweeping the reservoir rock; high efficiencies over a long period of time suggest conditions in which injection fluid can sweep heat from the reservoir while thermal front migration is less likely or takes longer to occur. Sweep efficiency is calculated for well pairs with sufficient data and plotted in Figure 8.

Thermal Front Migration

Within a geothermal reservoir, the velocity of a chemical tracer (fluid velocity) is greater than the velocity of a thermal front between production and injection well pairs. This is due to the heat capacity of the reservoir rock which buffers changes in temperature as cooler fluid is introduced into the reservoir. Using the mean residence time (first temporal moment (T*)) derived from tracer analysis, the timing of thermal change or thermal front migration can be estimated based on the relationship between water and rock temperatures in a geothermal reservoir.

For fluid flow through porous media, the ratio between the species and thermal velocities is given by Bodvarsson (1972):

$$\frac{V_{species}}{V_{thermal}} = \frac{(1-\varphi)\rho_r C_r + \varphi\rho_l C_l}{\varphi\rho_l C_l} \quad (1)$$

In this equation φ is the porosity, ρ is the density for liquid (l) or rock (r), and C is the heat capacity for liquid (l) and rock (r). Based on velocity and temporal moment of a tracer (Table 3) the thermal front ($T_{thermal}$) or breakthrough time is given by multiplying observed time by the velocity ratio:

$$T_{thermal} = T^* \left(\frac{V_{species}}{V_{thermal}}\right) \quad (2)$$

Using liquid and rock properties based on an assumed granitic geothermal reservoir and an average reservoir temperature of 250 °C , Equation (1) yields:

$$\frac{V_{species}}{V_{thermal}} = \frac{(1-\varphi) * 2700 * 0.79 + \varphi * 798.9 * 3.156}{\varphi * 798.9 * 3.156}$$

Due to the nature of permeability of a fault hosted system in hard granitic rock the connected porosity (permeable porosity) is likely different within the reservoir depending on where a well intersects the permeable zones with greater permeability being found directly within fault damage zones and permeability diminishing greatly within 1 – 2 meters away from the damage zone. As there is no direct measurement of the actual permeable porosity in this system a range of porosities (1%, 3%, 5%) were used to estimate possible thermal front migration times for injection and production well pairs. Using 1%, 3%, and 5% porosity and the assumed reservoir rock and water properties discussed above thermal velocity ratios are:

$$\frac{V_{species}}{V_{thermal}} = \frac{(1-0.01) * 2700 * 0.79 + 0.01 * 798.9 * 3.156}{0.01 * 798.9 * 3.156} = 85$$

$$\frac{V_{species}}{V_{thermal}} = \frac{(1-0.03) * 2700 * 0.79 + 0.03 * 798.9 * 3.156}{0.03 * 798.9 * 3.156} = 28$$

$$\frac{V_{species}}{V_{thermal}} = \frac{(1-0.05) * 2700 * 0.79 + 0.05 * 798.9 * 3.156}{0.05 * 798.9 * 3.156} = 17$$

Table 3 displays the $T_{thermal}$ values based on 1%, 3%, and 5% porosity for each production-injection well pair for which there was adequate data to evaluate T*.

Table 3. Summary of analytical tracer return evaluation for the geothermal field data. T* = mean residence time (first temporal moment), $T_{thermal}$ = thermal front migration time depending on assumed reservoir porosity, Vp = swept pore volume.

Injection Well	Production Well	T* residence time	$T_{thermal}$ (1% porosity)	$T_{thermal}$ (3% porosity)	$T_{thermal}$ (5% porosity)	V_p	Fracture Heterogeneity	Volumetric Sweep Efficiency	Remarks
		Days	Years	Years	Years	m^3			
I-1 (1,5 NDS)	P-1	Insufficient Data							No tracer decline observed
	P-2	120	27.8	9.3	5.6	242873	Moderate	Higher	
	P-3	129	29.9	10.0	6.0	599244	Moderate	Higher	
	P-4	158	36.7	12.3	7.4	1360963	Moderate	Higher	Low Confidence, $T^*>T_{total}$
	P-5	125	29.0	9.7	5.8	851383	Moderate	Higher	
I-2 (2,7 NDS)	P-1	Insufficient Data							No Tracer Returns
	P-2	Insufficient Data							No tracer decline observed
	P-3	Insufficient Data							No tracer decline observed
	P-4	196	45.5	15.2	9.2	222	Moderate	Higher	Low Confidence, $T^*>T_{total}$
	P-5	326	75.6	25.3	15.2	371	Higher	Higher	Low Confidence, $T^*>T_{total}$
I-3 (1 NS)	P-1	Insufficient Data							No Tracer Returns
	P-2	Insufficient Data							No tracer decline observed
	P-3	Insufficient Data							No Tracer Returns
	P-4	Insufficient Data							No tracer decline observed
	P-5	Insufficient Data							No Tracer Returns
I-4 (2,6 NDS)	P-1	100	23.2	7.8	4.7	211950	Lower	Higher	
	P-2	66	15.3	5.1	3.1	457593	Lower	Moderate	
	P-3	87	20.2	6.8	4.1	1093154	Higher	Lower	
	P-4	59	13.7	4.6	2.8	1438803	Moderate	Moderate	
	P-5	44	10.2	3.4	2.1	1036979	Moderate	Lower	

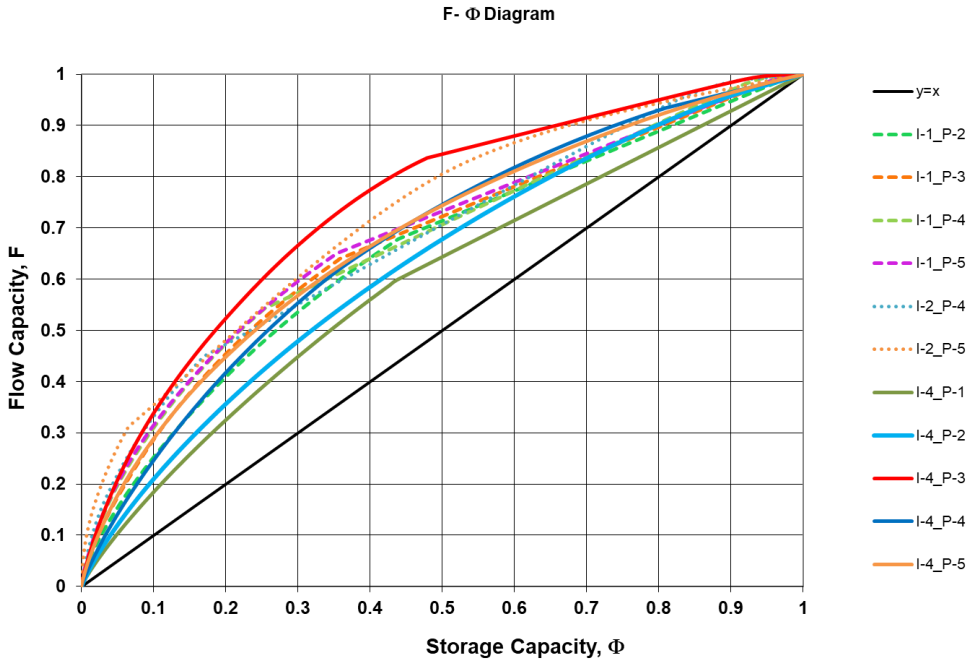

Figure 7. Flow-storage diagram for injection-production well pairs. The black line shows a 1:1 relationship between flow and storage capacity representative of flow through homogeneous porous media.

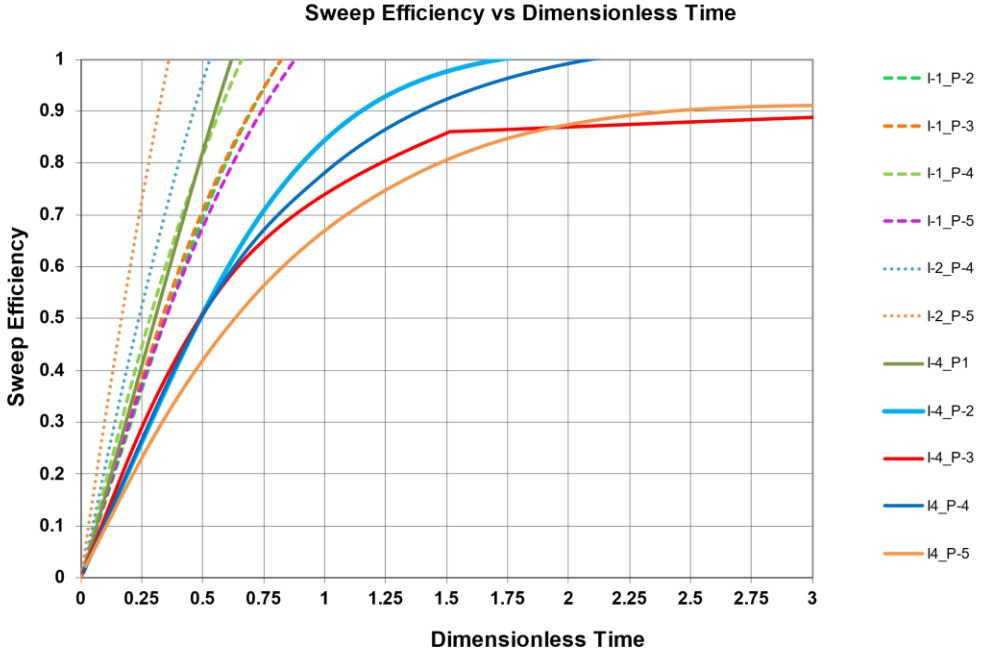

Figure 8. Sweep efficiency vs dimensionless time for injection-production well pairs. Dimensionless time is defined as the ratio of (t/t*) where t is time and t* is the thermal residence time defined in the text above.

Tracer Test Findings

General qualitative tracer findings are listed below:

- Tracer observation from injection wells I-4 and I-1 showed continual and recognizable patterns useful for further analytical analysis, while tracer returns from northern wells I-2 and I-3 were more sporadic (as were the injection rates) and likely do not represent true reservoir conditions for continual flow.
- Tracer returns from northern injection wells I-2 and I-3 confirm geothermal reservoir connection of these wells to the exploited geothermal reservoir which was previously unconfirmed.
- Tracer return times and magnitudes from injection wells can be summarized as follows:
    - Returns from I-4 in all production wells were observed between 6 – 30 days
    - Returns from I-1 in all production wells were observed between 11 – 47 days
    - Returns from I-3 in all production wells except P-1 were observed between 68 - 75 days
    - Returns from I-2 in all production wells except P-1 were observed between 7 - 75 days
- Maximum tracer return concentrations from I-4 were ~2X greater than I-1, 10X greater than I-3, and 20X greater than I-2.
- Tracers from all injection wells, except I-3, showed the same return timing pattern in production wells P-5 → P-4 → P-3 → P-2 → P-1.
- Tracer returns concentration patterns from injection wells I-4 and I-1 showed the same maximum tracer return concentration pattern with P-4 having highest concentration of all production wells followed by P-5 (P-4 → P-5 → P-3 → P-2 → P-1).

Based on the qualitative tracer findings above and tracer pair characteristics derived from temporal moment analysis of the tracer data the following conclusions may be drawn concerning the tested reservoir and related to the operational regime during the tracer testing period:

- Mean residence time (T*) values were ~20 – 100 days greater than peak tracer times indicating that flow paths in the geothermal reservoir generally are diffuse enough to allow time for water rock interaction and heat mining (heat transfer from rock to water) before being re-produced.
- Mean residence time (T*) for well pairs with injection well I-4 were 100 days or less indicating that I-4 has the fastest connection to production even though I-1 has a higher injection rate.
- The mean residence time (T*) for I-4 → P-5 is 44 days and showed the shortest initial and peak return time confirming that P-5 is very well connected to I-4 which is less than 1 km away and has only been producing at high rates for ~1 year. The relationship between these wells should be monitored closely as it is likely P-5 will see injection influence and possible cooling before any other well if high rates of injection are continued in I-4.
- Swept pore volumes for well pairs with I-4 and I-1 as the injector have the same general pattern with production wells P-2 and P-1 showing lower volumes than wells P-3, P-4, and P-5. The higher pore volumes were on the order of 800 thousand – 1.5 million cubic meters and the lower pore volumes were between 200 – 600 thousand cubic meters. This indicates production wells P-3, P-4, and P-5 see the greatest volumetric connection to injection and the exploited geothermal reservoir.
- Well pairs with northern injection wells I-2 have very low swept pore volumes (Vp = 222 and 371 cubic meters) compared the rest of the field and the highest residence times (T* = 196 and 326 days) indicating that the connection between the main portion of the reservoir and the northern injectors is very limited but does exist. Unfortunately, the operational data for I-2 (and I-3) indicate that injection to this well was not steady during the tracer period and the tracer return curves which can be analyzed using the Shook & Forsmann (2005) are sporadic meaning the values determined from this method are not robust and only give a qualitative representation of the likely connection between the northern injection wells and the main reservoir.
- The variation in flow geometry between well pairs is low. The most heterogenous well pair is I-4 → P-3, in which approximately 50% of the flow capacity is from 20% of the fracture network pore volume. Well pair I-4 → P-1 has the least heterogenous flow, in which approximately 50% of the flow capacity is from 35% of the fracture network pore volume. These results indicate that the geometry and flow paths of between different injection-production pairs are similar supporting the current conceptual

model which shows the geothermal reservoir permeability to be dominated by a single fault zone and associated fracture network.

- Injection-production pairs with I-1 and I-2 as the injector generally show high sweep efficiency over shorter time periods compared to well pairs with I-4 as the injector except for the pair I-4 → P-1. Well pairs I-4 → P-5 and I-4 → P-3 show much lower sweep efficiency over the same time periods indicating less pore volume is contacted during the same time periods possibly allowing for faster thermal front migration in those wells.

THERMAL FRONT MIGRATION DISCUSSION

Based on the tracer data analysis above the average $T_{thermal}$ times for well pairs in the main portion of the geothermal wellfield (I-1 or I-4 as injector) range from ~3 – 35 years with an average of ~11 years depending on assumed porosity which ranges from 1% - 5%. To investigate the timing of cooling of the geothermal system and evaluate the reliability of the thermal front migration calculations the average $T_{thermal}$ times are compared to observed cooling in the field based on static downhole temperature data where available.

It is important to note that the production wells came online for steady production at different times throughout the operational history of the field. Therefore, assessing cooling based on $T_{thermal}$ time estimates for injector-producer pairs must be based on specific well flow histories even as injection over time affects the reservoir as a whole. Furthermore, the average injection temperature changed from ~190°C to ~80°C in 2007 (binary unit online) allowing injection wells to accept more flow meaning initial cooling rates in the field were likely slower than the current operational regime when the tracer test was implemented. A comparison of historic flow data for the field up to the 2022 tracer period indicates the operational regimes during these times are reasonably comparable with I-1 taking the highest portion of injection field wide and production rates being similar though somewhat lower than historic levels in wells P-1, P-2, P-3, and P-4 as P-5 came online (Figure 9). This being the case the comparison of $T_{thermal}$ times estimated from tracer data to observed reservoir cooling in PT logs provide a reasonable first order comparison of temperature decline within the uncertainty associated with changes in wellfield operations. As I-4 injection has only been online since ~2018 and has had a relatively high degree of variation in flow during that time limits the level of confidence in the tracer results and estimated thermal front derived $T_{thermal}$ times related to this well.

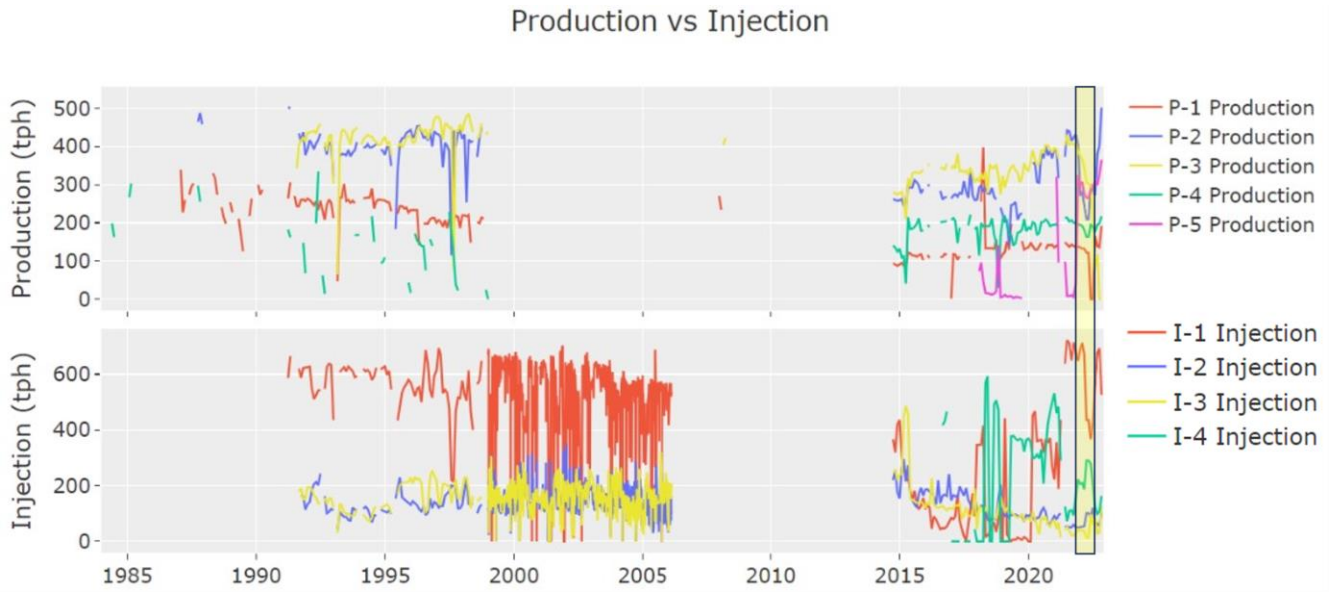

Figure 9. Available production and injection flow in metric tons per hour (tph) over time with the 2022 tracer test period highlighted. Missing flow data for production and injection datasets between ~2000 – 2015 is due to an issue with the electronic metering system at the power plant and historic data before ~2000 is generated from incomplete paper records.

Temperature Decline Comparison

Table 4 shows available temperature data for individual production wells along with start dates of steady production and temperature observation dates. Figure 10 shows a graphical representation of temperature decline in each well over time. If the pre-production reservoir temperature is assumed to be ~260 – 270°C, production wells P-3 and P-4 which have available temperature data to track decline over the time period after start up show a ~10 – 20 year buffer period where the reservoir temperature at that well is generally unchanged before temperature begins to decline. Production wells P-1 and P-2 which came online earliest in the field show faster temperature decline of ~1 – 4 years minimum however the initial decline timing and relative magnitude are difficult to constrain as there is minimal temperature log data available in the first 10 years of production. As production wells P-1 and P-2 have been operating consistently for much longer time periods the other production wells they also show the greatest degree of cooling to present (20 – 26°C).

Overall, when comparing the temperature decline pattern noted in Table 4 and Figure 10 to the average $T_{thermal}$ times derived from the 2022 tracer test (~3 – 25 years – 3% porosity), these align relatively closely with the measured temperature changes observed in the wellfield based on downhole temperature logs and are within the range of thermal front migration times based on 1 - 3% porosity. As is shown in in Figure 10 the observed temperature histories of this geothermal field generally fit the time scales of the tracer derived thermal front migration times when accounting for the relative uncertainty in exact fluid residence times based on the operational variation during the tracer test and reservoir porosity used in the thermal front calculations. In the case of P-1and P-2 for which tracer derived $T_{thermal}$ times are somewhat greater than the observed cooling this is likely due to P-1 and P-2 having relatively higher historic production rates compared to the rates during the tracer test period which would increase the speed on initial cooling especially in the early years of production when flow between producers and injectors was focused between I-1 and P-1/P-2 (Figure 9, Table 4, Figure 10). In the case of P-3 the 3% porosity $T_{thermal}$ time is ~10 years while the observed cooling does not take place for 20+ years which could be due to differences in the actual versus assumed porosity. If the porosity between I-1 and P-3 is taken to be ~1% then the $T_{thermal}$ time is greater than the observed at ~30 years indicating a porosity of ~2% may match the actual reservoir better (Table 3 and Table 4). The P-4 $T_{thermal}$ time based on 3% porosity is very close to the actual observed time of ~10 years (Table 4, Figure 10). P-5 has only been producing steadily for ~1 year but ~5°C of cooling has already been observed from the 2008 reservoir temperature post drilling (260°C) which is likely due to this well being affected cooling of the total reservoir due to long term production before P-5 came online. While the exact timing of observed temperature change in the field may differ on the order of few years from the predicted thermal front migration times the comparison shows that generally the tracer derived temperature decline provides a good first order estimate of the timing of cooling which could be better constrained with more specific estimates of porosity and more reliable tracer test operational settings in future.

As noted above the assumed porosity is an important factor in the thermal decline calculations and it appears an assumed porosity estimates of 3% provide the most comparable $T_{thermal}$ times for this geothermal field. While true measures of the porosity of a geothermal reservoir are difficult to obtain the assumption of 3% porosity for a highly productive field is well within typical reported porosity values for geothermal fields around the world and gives reasonable confidence in the first order temperature decline estimates (Moeck, 2014) (Rejeki et al., 2005). Therefore, based on the comparison above it appears that estimated $T_{thermal}$ times derived from tracer return data provide reasonable and useful estimates for temperature decline in this operating geothermal field.

Table 4. Available temperature data for individual production wells along with steady production start dates and temperature decline start dates. Note that the 3% Porosity Tracer Derived Thermal Front Migration Time for *P-1 is from tracer data from I-4 which was not online during the initial startup of P-1 but gives some sense (likely an overestimate) of the thermal front time for P-1 in compared to observed temperature change.

Well	Steady Production Start Date	Survey Date	Reservoir Temperature (°C)	Temperature Decline Start Date	Temperature Decline Buffer Length	3% Porosity Tracer Derived Thermal Front Migration Time (years)	Total Temperature Decrease (°C)
P-1	1985	8/17/1985	260	Post 1988	Minimum 3 years	*7.8 (I-4)	20
		6/9/1988	260				
		11/7/1997	250				
		7/9/2020	240				
P-2	1987	7/10/1987	262	Post 1988 - Pre 1992	Minimum 1 year - 4°C decrease after 5 years	9.3 (I-1)	26
		6/8/1988	261				
		9/19/1992	258				
		4/8/2010	257				
		4/8/2021	236				
P-3	1991	4/7/2012	263	Post 2012	~20 years	10.0 (I-1)	16
		4/8/2021	247				
P-4	2001	4/5/2012	263	Post 2012	~10 Years	12.3 (I-1)	17
		4/8/2021	246				
P-5	2018	4/18/2008 - *Pre-Production	260	Post 2008 - Reservoir already cooled from pre-2018 production start	Undetermined – Reservoir temperatures in the P-5 area were still ~260°C in 2008 after ~20 years of reservoir exploitation	9.7 (1-1) 3.4 (I-4)	5
		4/4/2018 - *Flowing Survey	256				
		7/10/2020	255				

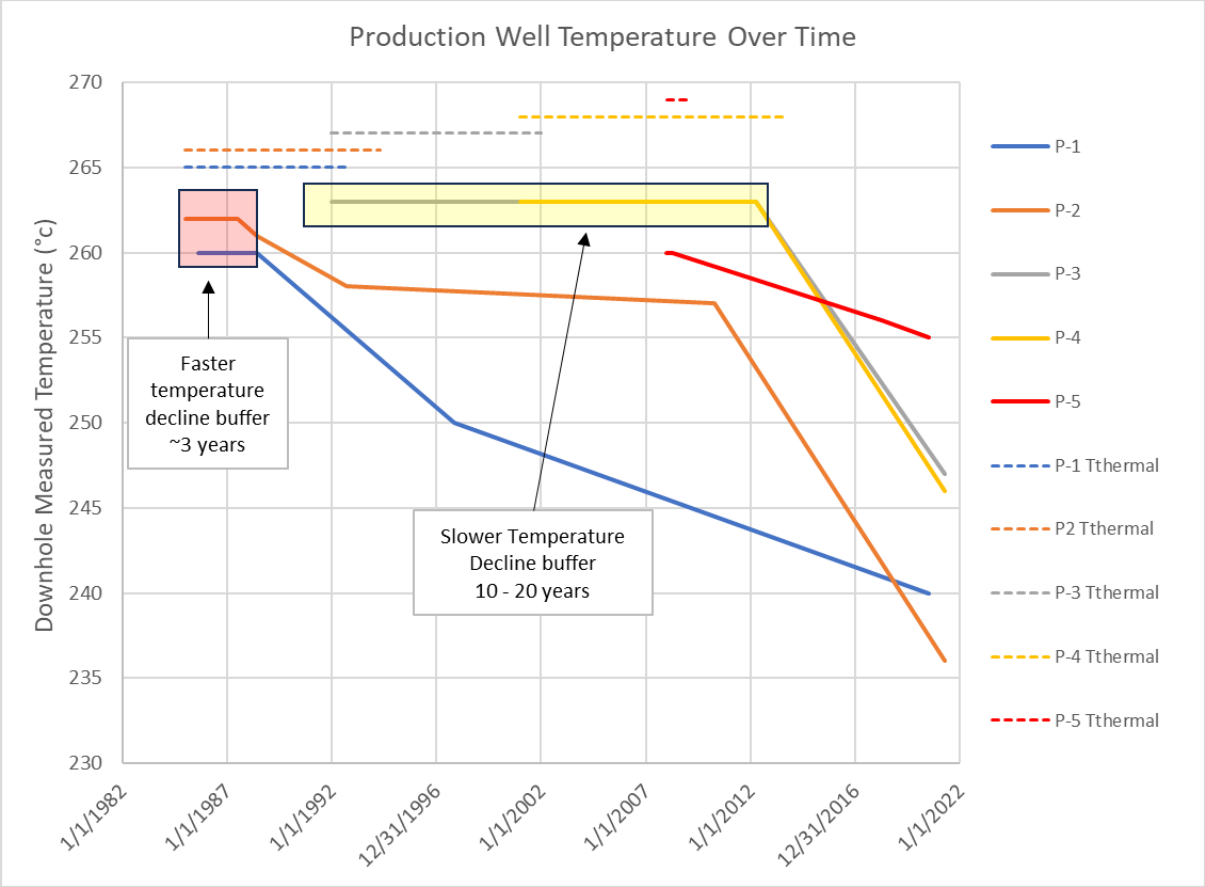

Figure 10. Graphical representation of temperature decline measured in production wells over time and $T_{thermal}$ times derived from tracer return data based on 3% assumed porosities. Temperature decline buffer periods discussed in the text are highlighted and annotated.

CONCLUSIONS AND OPERATIONAL IMPACTS

The results of the 2022 tracer test indicate production-injection well pairs in the main reservoir area (I-1,I-4) are well connected. Notably, the connection between the relatively recently drilled injection well I-4 and all operating production wells is fast and of high magnitude though with a relatively large swept pore volume which indicates a reservoir with enough surface area to currently sufficiently reheat injected fluid without causing detrimental thermal decline currently. A review of thermal front migration calculations based on tracer return data and compared to observed temperature decline shows these thermal decline times give a good first order estimate of when cooling may be observed at specific production wells. Since some cooling (~20 – 30°C) has currently been observed in the field, further tracking of this phenomenon will be critical to the long-term management of the reservoir as new wells I-4 and P-5 are operated over a longer time span. Tracer returns in production wells P-4 and P-5 from injection at I-4 show $T_{thermal}$ times of ~3 – 5 years based on 3% reservoir porosity and therefore could begin to see higher rates of thermal decline in the next few years depending on the injection and production rates at these wells. This being the case, considering options for moving greater volumes on injection out of the main field could be a good operational strategy over time especially as tracer data has confirmed the connection of northern injection wells I-2 and I-3 to the main reservoir. While thermal decline has been observed in the geothermal reservoir and the tracer data confirm that thermal effects from injection may be seen on the 3 – 10 year timescale it is important to note that the geothermal reservoir pressure and temperature decline over time has been relatively low compared to other Basin and Range fields with long production histories (Richards, 2022) and appears to likely has sufficient fuel reserves for many years to come. Other strategies which could be used to combat problematic cooling could be changing injection strategy back to greater rates at I-1 which has overall slower connections to current production wells and or retooling some production wells to be injectors such as P-1 which is well connected to the main reservoir but is located farther from the outflow and main production center near P-3, P-4, and P-5.

REFERENCES

Bodvarsson G.: Thermal Problems in Siting of Reinjection Wells. Proceedings, Geothermics, (1972), 63-66

Moeck, I.: Catalog of geothermal play types based on geologic controls. Renewable and Sustainable Energy Reviews 37, (2014), 967-882

Rejeki, S., Hadi, J., Suhayati, I.: Porosity Study for Detail Reservoir Characterization in Darajat Geothermal Field, West Java, Indonesia. Proceedings World Geothermal Congress, (2005)

Richards, M.: Geothermal Energy, *in*, The Nevada Mineral Industry 2022: NBMG Special Publication MI (2022), 56-70

Shook, G.M.: Predicting Thermal Breakthrough in Heterogeneous Media from Tracer Tests, Geothermics, (2001), 573-589

Shook, G.M., and Forsmann, J.H.: Tracer Interpretation Using Temporal Moments on a Spreadsheet, Idaho National Laboratory, Geothermal Technologies Program, Idaho Falls, Idaho (2005), 573-589